Pt- and K-promoted supported gallia as a highly stable alternative catalyst for isobutane dehydrogenation

Anna N. Matveyeva,[a] Nadezhda A. Zaitseva,[b] Nikolai A. Pakhomov,[c] and Dmitry Yu. Murzin*[d]

[a] A. N. Matveyeva
Laboratory of Materials and Processes for Hydrogen Energy
Ioffe Institute
Politekhnicheskaya ul. 26, St. Petersburg 194021, Russia
[b] N. A. Zaitseva
Boreskov Institute of Catalysis SB RAS
Prospekt Akademika Lavrentieva 5, Novosibirsk 630090, Russia
[c] Dr. N. A. Pakhomov
Laboratory of Catalytic Technologies
St. Petersburg State Institute of Technology (Technical University)
Moskovsky pr. 26, St. Petersburg 190013, Russia
[d] Prof. D. Yu. Murzin
Laboratory of Industrial Chemistry and Reaction Engineering
Åbo Akademi University
Biskopsgatan 8, Turku/Åbo 20500, Finland
E-mail: dmurzin@abo.fi

Supporting Information

Experimental Section

Catalysts preparation

Powdered aluminum precursor supplied by FOR-ALUMINA (Russia) was obtained from gibbsite under the following conditions: heating surface temperature 620 °C; reagent mass flow 175 kg/h. It had the following properties, which were determined using N_2 physisorption: specific surface area – 295 m^2/g; total pore volume – 0.21 cm^3/g; average pore diameter – 2.4 nm. The particle size of alumina was in the range 40–100 μm.

Preparation of the catalysts was done using capillary impregnation of the alumina precursor by a slow dropwise addition of aqueous solutions of $Ga(NO_3)_3 \cdot 9H_2O$, $H_2[PtCl_6] \cdot 6H_2O$ and KOH under vigorous stirring in the quantities depending of the target loadings, drying the impregnated solid at 90–110 °C for 2 h and then calcination at 650–750 °C for 4 h in static air. To simplify the catalyst preparation, the impregnation was carried out on the alumina precursor rather than on alumina itself, as no differences in catalytic properties were observed for the latter case. The gallium content was 1.5, 3 and 6 wt. %, platinum – 0.01, 0.05 and 0.1%, potassium – 0.25 and 1.25%.

Characterization

The phase composition of the samples was determined by the powder X-ray diffraction (XRD) on XRD-6100 (Shimadzu, Japan) at the following conditions: CuKα-radiation (Ni-filter), 40 kV voltage, 30 mA current, 2°/min scan speed, 0.02° step width, 3.6 s exposition, 20–55° 2θ scan range; divergence (D), scattering (S) and receiving (R) slits – D:S:R = 1:1:0.3.

Textural and structural properties were determined by performing N_2 physisorption at –196 °C using an Autosorb-6iSA (Quantachrome Instruments, USA). Prior to the measurements the samples (0.1–0.2 g) were degassed at 250 °C under vacuum up to residual pressure 12 Pa for 1 h. The specific surface area was calculated by the MultiPoint BET (Brunauer, Emmett, Teller) method. The presence of micropores was determined using the Alpha-S (α_s) method. The pore size distribution was calculated by DFT (Density Functional Theory) method. It is now becoming more and more evident that the pore size analysis of narrow mesopores cannot be reliably achieved by procedures based on the Kelvin equation, such as the Barrett-Joyner-Halenda (BJH) method.

The morphology of samples was studied via scanning electron microscopy (SEM) using a TESCAN VEGA 3 SBH microscope. Energy dispersed X-ray analysis (EDX) was performed in the same microscope using Oxford instruments INCAx-act.

The Brønsted and Lewis acid sites were measured by infrared spectroscopy (ATI Mattson FTIR, LabX) using pyridine as a probe molecule. A thin self-supported wafer of a sample was pressed (about 15–25 mg at 2 tons pressure for 5 min) and then placed into the FTIR-cell. The cell was evacuated and the temperature was raised to 450 °C and kept for 1 h. Thereafter, the temperature was decreased to 100 °C and the background spectra of a sample were recorded. Pyridine was adsorbed first for 30 min at 100 °C followed by desorption at 250, 350 and 450 °C for 1 h for determination of weak, medium and strong acid sites. The spectra of the sample were recorded in between every temperature ramp. Scanning was performed under vacuum at 100 °C. Spectral bands at 1545 cm^{-1} and

at 1450 cm^{-1} were used to identify Brønsted (BAS) and Lewis (LAS) acid sites, respectively. The quantitative amount of BAS and LAS was calculated with the constants of Emeis.

The functionality of samples was studied using selective adsorption from their aqueous solutions of a series of acid-base indicators with different intrinsic pK_a values in the range from −4.4 to 14.2 on the surface sites with the corresponding pK_a values resulting in the change of the indicator solution optical density. Another factor contributing to the optical density change is the change of the aqueous medium acidity as a result of water interactions with the surface sites. For this reason, the performed analysis involved spectrophotometric measurements (using a spectrophotometer UV-1800 (Shimadzu)) of the following optical density (D) values: D_0 – for the initial aqueous solution of the indicator of a certain concentration; D_1 – for the same solution containing a sample of the analyzed compound of a certain weight where both the indicator adsorption and pH change affect the optical density; D_2 – for the same solution added to the solvent (water) decanted after the contact with a sample of the same weight. In this case, the optical density is affected only by pH value changed due to solvent (water)–surface interactions. This factor can be eliminated using the following approach. The measurements described above allow evaluation of adsorption sites with a certain pK on the studied surface according to the following equation:

$$Q(pK_a) = \left| \frac{|D_0 - D_1|}{m_1} \pm \frac{|D_0 - D_2|}{m_2} \right| \cdot C_{ind} \cdot V_{ind} / D_0 , \quad (1)$$

where C_{ind} is the concentration of the indicator solution; V_{ind} is the volume of the indicator solution used in the analysis; m_1 and m_2 are weights of the samples for measuring D_1 and D_2 correspondingly; «+» sign corresponds to the case where D_1 and D_2 are oppositely changed related to D_0 ($D_1<D_0$ and $D_2>D_0$, i.e. the changes in optical density caused by adsorption and water-surface interactions are opposite and the decrease of optical density due to the indicator adsorption is larger than the increase due to the water-surface interactions); «–» sign corresponds to unidirectional optical density changes

caused by both adsorption and water-surface interactions ($D_1<D_0$ and $D_2<D_0$, i.e. either water-surface interactions results in the decrease of the optical density or they result in an increase of this value but a decrease caused by adsorption is more prominent).

The indicators used in this study and their parameters are presented below:

№	Indicator	pK_a	Wavelength λ (nm)	Volume V_{ind} (mL)	C_{ind} (mmol/L)
1	Ethylene glycol	14.2	200	0.3	Concentrated
2	Indigo-carmine	12.8	610	0.5	0.40
3	Nile blue	10.5	640	0.1	0.37
4	Tymol blue	8.8	430	0.5	0.41
5	Bromo-tymol blue	7.3	430	0.5	0.36
6	Bromo-crezyl purple	6.4	590	0.5	0.16
7	Methyl red	5.0	430	0.2	0.37
8	Bromo-phenol blue	4.1	590	0.2	0.10
9	Methyl orange	3.5	460	0.5	0.21
10	m-Nitroaniline	2.5	340	1.0	1.81
11	Fuccine	2.1	540	0.3	0.15
12	Brilliant green	1.3	610	0.1	0.31
13	Crystalline violet	0.8	580	0.5	0.12
14	o-Nitroaniline	-0.3	410	0.5	1.09
15	p-Chloro-nitroaniline	-0.9	330	1.0	0.45
16	Dinitroaniline	-4.4	340	1.0	1.20

The total surface acidity was determined by the temperature-programmed desorption (TPD) of NH_3 at ambient pressure with an AutoChem 2910 instrument from Micromeritics with a thermal conductivity detector (TCD), which is capable of detecting minute differences in the concentration of gases, and a cooling equipment KwikCool (Micromeritics). The following procedures were applied during the pre-treatment:

- A certain amount (0.17 g) of a powder sample was placed in an adsorption vessel (U-shaped reactor) a top a quartz wool layer into the thermocouple zone. For the purpose of removing water vapor or other adsorbed pollutants, the sample was preheated to 550–850 °C with a ramp of 10 °C/min under a 20 cm^3/min He flow (99.996 vol. % He) and held under those conditions for 1 h, followed by cooling to 100 °C with a ramp of 10 °C/min and holding for 1 h.

- For NH_3 adsorption 20 cm^3/min of 5 vol. % NH_3 in He was injected for 1 h at 100 °C to saturate the sample, followed by purging with He (20 cm^3/min) for 1 h to remove physically adsorbed forms from the surface.

- TPD of NH_3 was recorded during heating to the calcination temperature at a ramp of 10 °C/min and constant helium flow rate (20 cm^3/min).

- The concentration of the acid sites was determined using the following equation:

$$n_s = \frac{\frac{S_2}{S_1} \cdot n_{NH_3}}{m_{cat}}, \quad (2)$$

where n_s – acidity of the sample, mmol/g; S_2 – NH_3 peak area; S_1 – 1 ml 5 vol. % NH_3 peak average area; n_{NH_3} – $2.02 \cdot 10^{-3}$ (at 28.5 °C), mmol; m_{cat} – sample mass, g.

Catalytic tests

The catalytic behavior of the prepared catalysts was studied in an automated laboratory scale unit at atmospheric pressure. A cylindrical quartz tube, 200 mm in length, 15 mm in inner diameter was used as a reactor in which the catalyst was placed on a heat-resistant porous filter made of SiO_2. The reactor contained a pocket for the thermocouple with an external diameter of 5 mm. Fluidization was ensured by an upstream flow of the reacting gas. When the gas was supplied in the opposite direction, the reactor operated in a fixed-bed mode. The heat supply was provided by placing the reactor in an oven operating at a desired temperature.

The experiments were carried out in a cyclic mode for 16th or more successive dehydrogenation-regeneration cycles with a catalyst loading of 5 cm^3 in the case of a fluidized-bed and 0.5 cm^3 (diluted with 1 cm^3 of quartz) in the case of a fixed-bed reactors.

A standard duration of dehydrogenation was 10 min at 580 °C, and the regeneration by air was no more than 30 min at 650 °C. In some experiments, the dehydrogenation proceeded for 3 hours. The

regeneration and dehydrogenation stages are separated from each other by purging with helium (10–15 min) for safety reasons. The isobutane purity was > 99.9 vol. %.

The initial gases and reaction products were analyzed on a Khromos GKh-1000 chromatograph with a flame-ionization detector (FID) and 30-m SiO_2 capillary column operating at 100 °C. In 10 min after the start of the reaction, the test sample was taken from a gas flow by automatically turning the sampling valves. The peak areas were used in the calculations taking into account the relevant response factors.

The content of hydrogen was not taken into account.

Isobutane conversion, isobutene yield and selectivity to isobutene were calculated as:

$$X = (i\text{-}C_4H_{10}^{in} - i\text{-}C_4H_{10}^{out})/i\text{-}C_4H_{10}^{in}, \quad (3)$$

$$Y = i\text{-}C_4H_8^{out}/i\text{-}C_4H_{10}^{in}, \quad (4)$$

$$S = Y/X, \quad (5)$$

where $i\text{-}C_4H_{10}^{in}$ and $i\text{-}C_4H_{10}^{out}$ are the mass content of isobutane in the feed and the exit flows respectively, $i\text{-}C_4H_8^{out}$ is the isobutene mass content in the exit flow.

The mass balance closure taking into account also the amount of generated coke was ca. 99–100%.

The coke content was calculated by the amounts of CO and CO_2 released during regeneration, which were recorded by a TEST gas analyzer (BonAir Ltd) having an optical-absorption infrared sensor. Analysis of the output concentrations of CO and CO_2 by these sensors allowed calculating the amount of coke deposits.

The coke yield was determined by the following equations:

$$Y_{coke} = \frac{V_{CO_x}}{4W \cdot T} \cdot 100, \quad (6)$$

$$V_{CO_x} = U \cdot \int_0^t C_{CO_x} dt \quad , \tag{7}$$

where Y_{coke} – the coke yield, wt. %; W – flow rate during the reaction, L/h; U – flow rate during the regeneration, L/h ; T – reaction time, h; V_{CO_x} – volume of the evolved CO_x for regeneration, L; C_{CO_x} – molar fraction of CO_x in the stream.

The observed reaction rate or the rate of converted isobutane (mmol/h/g) was calculated as:

$$r(i\text{-}C_4H_{10}) = n(i\text{-}C_4H_{10}) \cdot X/m_{cat}, \tag{8}$$

where $n(i\text{-}C_4H_{10})$ – inlet molar flow of isobutane, mmol/h; m_{cat} – mass of the catalyst, g.

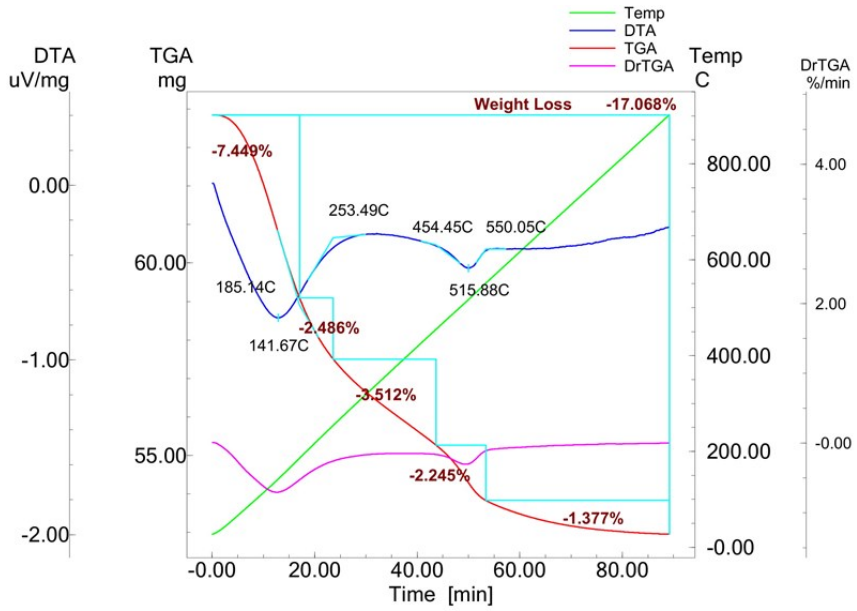

Figure S1. TGA and DTA data for the support.

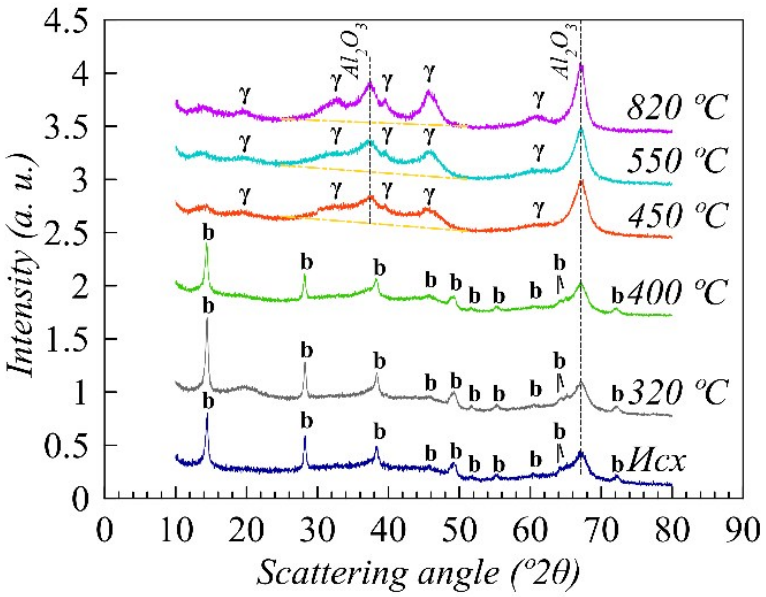

Figure S2. XRD patterns for the alumina support calcined at different temperatures (b – boehmite; γ – γ-Al_2O_3).

Table S1. Textural properties of the support and catalysts.

Sample	$S_{sp.}$ (m^2/g)	$\sum V_{p.}$ (cm^3/g)	$d_{p.}$ (nm)	LAS (μmol/g)/(μmol/m^2)			BAS (μmol/g)
				Weak	Medium	Strong	Total
Al_2O_3-750	143	0.26	5.7	-	-	-	-
3Ga-750	123	0.24	6.1	10/0.0081	0	0	0
3Ga-0.25K-750	121	0.32	6.6	8/0.066	0	0	0
3Ga-0.1Pt-750	-	-	-	12/0.099[b]	0	0	0
3Ga-0.1Pt-0.25K-750[a]	140	0.26	6.1	8/0.057	0	0	0
Note: [a] Prepared on another batch of support; [b] – under the assumption that the specific surface as for 3Ga-0.25K-750; $S_{sp.}$ – specific surface area of sample; $\sum V_{p.}$ – total pore volume; $d_{p.}$ – average pore diameter.							

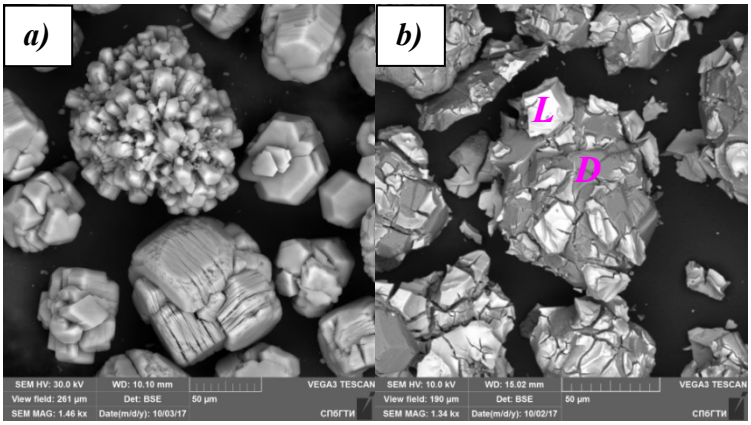

Figure S3. SEM images of a) calcined support b) 9Ga-650, where L – light area, D – dark area.

Table S2. EDX results for different areas of 6Ga-700 catalyst.

wt. %	O	Al	Ga
dark area	47.6	46.1	6.3
light area	37.9	25.6	36.6

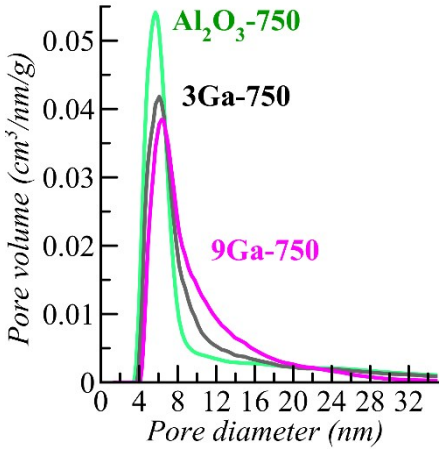

Figure S4. Pore size distribution of the calcined support, 3Ga and 9Ga at 750 °C.

Table S3. Conversion (X, %), selectivity to isobutene (S, %) and coke yield (C, %) obtained in several cycles of dehydrogenation in a fluidized-bed of Ga, Pt and K-supported catalysts at 580 °C.

Components supported on Al_2O_3 (wt. %)	Feed and velocity (L/h)	GHSV based on i-C_4H_{10} (feed)	After 1st cycle			After 16th cycle			After end cycle			
			X	S	C	X	S	C	№	X	S	C
Fluidized-bed												
6Ga-700 (m = 6.00 g)	i-C_4H_{10} = 2.0	400	48	68	2.3	46	69	1.8	58	46	69	1.8
6Ga-1.25K-700	i-C_4H_{10} = 2.0	400	-	-	-	25	86	-	-	-	-	-
3Ga-650 (m = 5.65 g)	i-C_4H_{10} = 2.0	400	42	65	2.1	45	67	2.0	-	-	-	-
3Ga-0.1Pt-750 (m = 5.80 g)	i-C_4H_{10} = 2.0	400	65	70	2.9	64	69	2.7	28	63	70	2.5
	i-C_4H_{10}:H_2 = 2.0:0.5	400 (500)	-	-	-	61[a]	69[a]	1.7[a]	98	67	70	1.3
3Ga-0.01Pt-750 (m = 6.36 g)	i-C_4H_{10}:H_2 = 2.0:0.5	400 (500)	56	74	1.1	58	69	1.4	-	-	-	-
1.5Ga-0.05Pt-	i-C_4H_{10}:H_2 =	400	61	71	1.1	61	71	1.1	-	-	-	-

750 (m = 6.35 g)	2.0:0.5	(500)										
3Ga-0.1Pt-0.25K-750 (m = 6.28 g)	i-C_4H_{10} = 2.0	400	-	-	-	-	-	-	322	63	83	0.7
	i-C_4H_{10}:H_2 = 2.0:0.5	400 (500)	61	78	1.3	60	79	0.6	305	59	82	0.5
3Ga-0.05Pt-0.25K-750 (m = 6.17 g)	i-C_4H_{10} = 2.0	400	-	-	-	50[a]	83[a]	0.8[a]	199	63	83	0.6
	i-C_4H_{10}:H_2 = 2.0:0.5	400 (500)	58	83	0.8	60	80	1.0	309	59	83	0.3
Fixed-bed (weight of the catalyst = 0.65 g)												
3Ga-0.25K-750	i-C_4H_{10}:H_2 = 1.0:0.5	2000 (2100)	19	86	0.1	25	89	0.1	-	-	-	-
0.1Pt-0.25K-750	i-C_4H_{10}:H_2 = 1.0:0.5	2000 (2100)	16	77	0.1	10	75	0.0	-	-	-	-
3Ga-0.1Pt-0.25K-750	i-C_4H_{10}:H_2 = 1.0:0.5	2000 (2100)	58	88	0.3	55	92	0.2	-	-	-	-
3Ga-0.01Pt-0.25K-750	i-C_4H_{10}:H_2 = 1.0:0.5	2000 (2100)	53	94	0.2	54	94	0.1	128	54	94	0.1
Note: [a] After 19th cycle.												

Table S4. Product distribution in isobutane dehydrogenation over Ga, Pt and K-supported catalysts at 580 °C.

Time	CH_4	C_2H_6	C_2H_4	C_3H_8	C_3H_6	n-C_4H_{10}	1-C_4H_8	t-2-C_4H_8	i-C_4H_8	c-2-C_4H_8
3Ga-0.1Pt-0.25K-750 (fluidized-bed; i-C_4H_{10}=2 L/h; 400 h^{-1})										
10	2.76	0.69	0.05	4.46	2.24	2.57	1.14	1.28	83.99	0.82
60	3.00	0.56	0.08	4.29	2.93	2.46	1.38	1.56	82.70	1.05
120	3.57	0.48	0.15	3.35	4.11	1.28	1.30	1.45	83.32	0.98
180	3.97	0.46	0.19	3.00	4.69	0.99	1.31	1.43	83.03	0.93
3Ga-0.1Pt-0.25K-750 (fluidized-bed; i-C_4H_{10}:H_2=2.0:0.5 L/h; 2100 h^{-1})										
10	2.63	0.61	0.04	4.51	2.07	3.04	1.19	1.37	83.65	0.88
60	3.00	0.56	0.08	4.29	2.93	2.46	1.38	1.56	82.70	1.05
120	3.22	0.53	0.11	4.02	3.44	2.06	1.43	1.59	82.54	1.06
3Ga-0.1Pt-0.25K-750 (fluidized-bed; i-C_4H_{10}=2 L/h; 400 h^{-1})										
10	3.34	0.43	0.13	3.65	4.27	1.26	1.23	1.17	83.73	0.80
60	4.32	0.42	0.31	2.97	6.46	0.81	1.47	1.45	80.77	1.01
120	4.37	0.36	0.33	0.35	6.49	0.66	1.47	1.46	83.53	0.99
180	4.45	0.34	0.33	2.51	6.39	0.57	1.38	1.35	81.75	0.94
3Ga-0.05Pt-0.25K-750 (fluidized-bed; i-C_4H_{10}:H_2=2.0:0.5 L/h; 2100 h^{-1})										
10	2.72	0.35	0.05	3.93	2.75	1.65	0.98	1.03	85.92	0.63
60	3.47	0.46	0.15	3.78	4.46	1.50	1.43	1.54	82.20	1.02
120	3.80	0.47	0.22	3.56	5.17	1.33	1.55	1.66	81.13	1.11
180	3.30	0.43	0.13	3.65	4.28	1.26	1.23	1.17	83.76	0.80

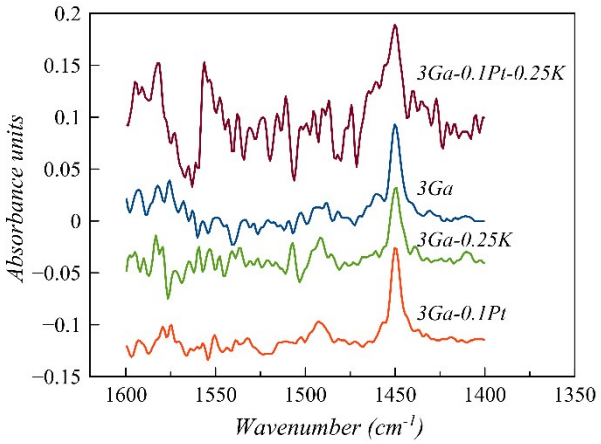

Figure S5. Spectra of adsorbed pyridine on catalysts.

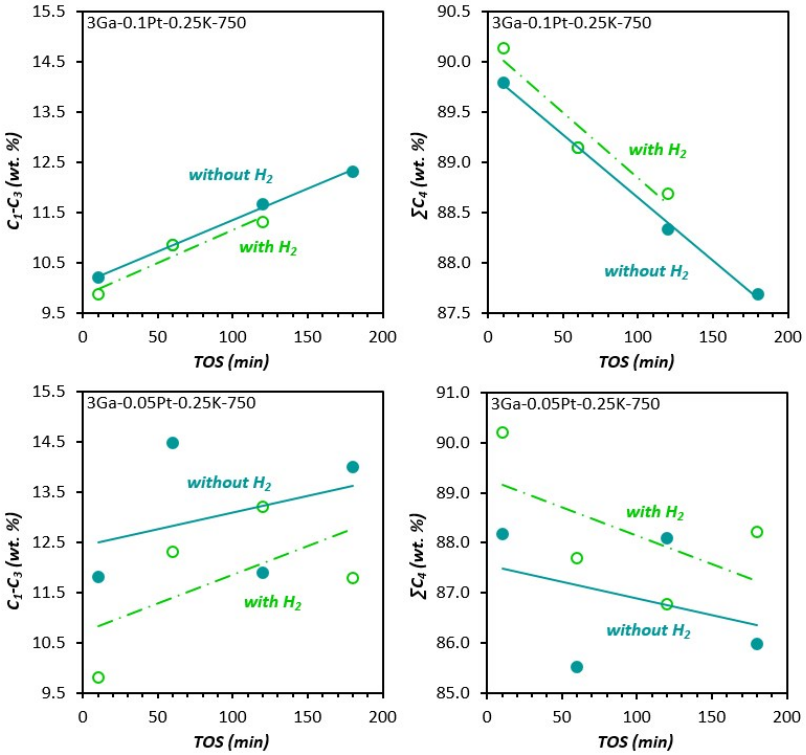

Figure S6. C_1–C_3 and C_4 fractions in the presence and absence of H_2.